

Minor Structural Variations of Small Molecules Tune Regulatory Activities toward Pathological Factors in Alzheimer's Disease

Michael W. Beck,^[a, b] Jeffrey S. Derrick,^[a] Jong-Min Suh,^[a] Mingeun Kim,^[a] Kyle J. Korshavn,^[b] Richard A. Kerr,^[b] Woo Jong Cho,^[c] Scott D. Larsen,^[d] Brandon T. Ruotolo,^[b] Ayyalusamy Ramamoorthy,^{*[b, e]} and Mi Hee Lim^{*[a]}

Chemical tools have been valuable for establishing a better understanding of the relationships between metal ion dyshomeostasis, the abnormal aggregation and accumulation of amyloid- β (A β), and oxidative stress in Alzheimer's disease (AD). Still, very little information is available to correlate the structures of chemical tools with specific reactivities used to uncover such relationships. Recently, slight structural variations to the framework of a chemical tool were found to drastically determine the tool's reactivities toward multiple pathological facets to various extents. Herein, we report our rational design and characterization of a structural series to illustrate the extent to which the reactivities of small molecules vary toward different

targets as a result of minor structural modifications. These compounds were rationally and systematically modified based on consideration of properties, including ionization potentials and metal binding, to afford their desired reactivities with metal-free or metal-bound A β , reactive oxygen species (ROS), and free organic radicals. Our results show that although small molecules are structurally similar, they can interact with multiple factors associated with AD pathogenesis and alleviate their reactivities to different degrees. Together, our studies demonstrate the rational structure-directed design that can be used to develop chemical tools capable of regulating individual or interrelated pathological features in AD.

Introduction

Effective diagnostic tools and treatments for neurodegenerative diseases have been unavailable to date due to multiple aspects. One reason is the lack of our understanding of the underlying pathogenesis required to develop such medical interventions.^[1] This is highlighted in Alzheimer's disease (AD) where, despite being one of the better-studied neurodegenerative diseases, the etiology is still unclear.^[1] The current understanding of AD implicates multiple factors that could be interrelated.^[1a-c,e,g,2] Recently, an area of particular high interest is

the interconnection between metal ion dyshomeostasis, the abnormal aggregation and accumulation of an intrinsically disordered protein (IDP) [i.e., amyloid- β (A β)], and increased oxidative stress in the brain. Metal ions have been suggested to be central to this interrelationship as several biologically relevant metal ions [e.g., Fe^{II/III}, Cu^{I/II}, Zn^{II}] have been shown in vitro to bind to A β and influence its aggregation and conformation.^[1a-c,e,2a-e] Additionally, the coordination of A β to redox-active metal ions, Fe^{II/III} and Cu^{I/II}, has been shown to facilitate the production of reactive oxygen species (ROS) through Fenton-like reactions.^[1a-c,e,2a-c,e,3]

To elucidate this interrelationship in depth, chemical tools have been developed to target individual or interrelated factors and modulate their reactivities.^[1a,b,4] These tools and potential therapeutics include approaches that use organic, inorganic, peptide, and antibody frameworks.^[1a-c,e-h,4] We recently reported the development of four small molecules (1–4; Table 1) which have different modes of action, despite being structurally similar, for targeting and controlling the aggregation of metal-free A β or metal-A β as well as the formation of ROS overall diminishing toxicity.^[5] Herein, we report the overall investigations of the small molecules (1–9; Table 1) rationally designed to tune the reactivities with differing targets (i.e., metal ions, metal-free A β , metal-A β , ROS, free organic radicals) by performing slight structural modifications to a common structural framework. Through chemical, biochemical, biophysical, and computational studies, we demonstrate that 1–9 have

[a] Dr. M. W. Beck, J. S. Derrick, J.-M. Suh, M. Kim, Prof. Dr. M. H. Lim
Department of Chemistry, Ulsan National Institute of Science and Technology (UNIST), Ulsan 44919 (Republic of Korea)
E-mail: mhlum@unist.ac.kr

[b] Dr. M. W. Beck, Dr. K. J. Korshavn, Dr. R. A. Kerr, Prof. Dr. B. T. Ruotolo,
Prof. Dr. A. Ramamoorthy
Department of Chemistry, University of Michigan, Ann Arbor, MI 48109
(USA)
E-mail: ramamoor@umich.edu

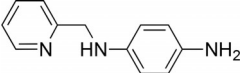
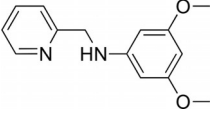
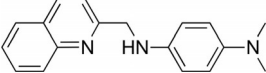
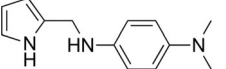
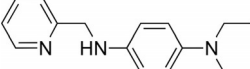
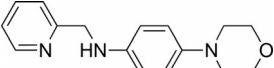
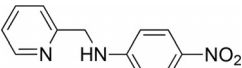
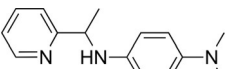
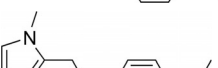
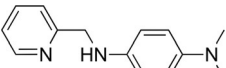
[c] Dr. W. J. Cho
School of Life Sciences, Ulsan National Institute of Science and Technology
(UNIST), Ulsan 44919 (Republic of Korea)

[d] Prof. Dr. S. D. Larsen
Department of Medicinal Chemistry, University of Michigan, Ann Arbor, MI
48109 (USA)

[e] Prof. Dr. A. Ramamoorthy
Biophysics Program, University of Michigan, Ann Arbor, MI 48109 (USA)

Supporting information and the ORCID identification number(s) for the author(s) of this article can be found under:
<https://doi.org/10.1002/cmdc.201700456>

Table 1. Structures of the small molecules designed to modulate reactivities of metal-free and metal-bound A β and oxidative stress, their first and second ionization potentials (IP₁ and IP₂), first peak anodic potentials (E_{pa1}), Trolox equivalent antioxidant capacity (TEAC), and reactivities with metal-free A β , Cu^{II}-A β , and Zn^{II}-A β .

Compound ^[a]	IP ₁ [eV]	IP ₂ [eV]	E_{pa1} [V]	TEAC	A β Reactivity ^[b]		
					Metal-free	Cu ^{II}	Zn ^{II}
	6.23 ^[5]	6.02 ^[5]	0.262	2.6 ± 0.2 ^[5]	×	✓	×
	6.76 ^[5]	7.16 ^[5]	0.923	1.6 ± 0.2 ^[5]	×	✓	×
	5.90 ^[5]	6.13 ^[5]	0.284	2.0 ± 0.2 ^[5]	×	✓	✓
	6.07 ^[5]	6.01 ^[5]	0.240	2.5 ± 0.2 ^[5]	✓	✓	✓
	5.82	5.91	0.228	1.5 ± 0.1	×	✓	✓
	6.06	6.02	0.388	3.2 ± 0.3	×	✓	×
	7.75	8.16	–	–0.1 ± 0.1	×	×	×
	6.01	5.83	0.286	2.0 ± 0.1	×	✓	✓
	6.10	6.06	0.238	1.8 ± 0.2	×	✓	✓
L2-b 	5.92 ^[8]	6.13 ^[8]	–	2.3 ± 0.2 ^[8]	×	✓	✓

[a] **1** = *N*¹-(pyridin-2-ylmethyl)benzene-1,4-diamine; **2** = 3,5-dimethoxy-*N*-(pyridin-2-ylmethyl)aniline; **3** = *N*¹,*N*¹-dimethyl-*N*²-(quinolin-2-ylmethyl)benzene-1,4-diamine; **4** = *N*¹-((1*H*-pyrrol-2-yl)methyl)-*N*⁴,*N*⁴-dimethylbenzene-1,4-diamine; **5** = *N*¹,*N*¹-diethyl-*N*²-(pyridin-2-ylmethyl)benzene-1,4-diamine; **6** = 4-morpholino-*N*-(pyridin-2-ylmethyl)aniline; **7** = 4-nitro-*N*-(pyridin-2-ylmethyl)aniline; **8** = *N*¹,*N*¹-dimethyl-*N*²-(1-(pyridin-2-yl)ethyl)benzene-1,4-diamine; **9** = *N*¹,*N*¹-dimethyl-*N*²-((1-methyl-1*H*-imidazol-2-yl)methyl)benzene-1,4-diamine; **L2-b** = *N*¹,*N*¹-dimethyl-*N*²-(pyridin-2-ylmethyl)benzene-1,4-diamine. [b] ×: No significant reactivity was observed.

structure-dependent capabilities to modulate the reactivities with their targets. The target specificity of these compounds (i.e., reactivity directed toward metal-free A β and/or metal-A β) have been indicated to be associated with their redox properties.^[5] 1) The compounds that undergo oxidation relatively easily suppress the reactivity of metal-A β over metal-free A β (**1**, **3**, **5**, **6**, **8**, and **9**) or both metal-free and metal-bound A β (**4**); 2) the compounds (**2** and **7**) that are more difficult to oxidize indicate limited abilities to control the reactivity of A β in the absence and presence of metal ions. In addition, the activity of our small molecules toward metal [Cu^{II} or Zn^{II}]-A β was indicated to be correlated to the formation of compound-metal-A β ternary complexes. In particular, with respect to interactions with Zn^{II}-A β , the metal binding affinity of the compounds for Zn^{II} was found to be critical for promoting such reactivity. Moreover, the activity of **4** with both metal-free A β and metal-A β could be linked to its degradation to a known A β modula-

tor, *N,N*-dimethyl-*p*-phenylenediamine (**DMPD**).^[6] Taken together, our studies presented herein demonstrate the feasibility of developing chemical tools toward individual or interrelated pathological factors in AD, through considerations of the electrochemical, metal binding, and biological properties of a series of structurally similar molecules to generate a rational structure-directed design approach. The insight gained from these studies, particularly those relating the redox properties of our small molecules to their anti-amyloidogenic activity will open new, innovative approaches to devise new chemical reagents able to target and mitigate specific or intercommunicated pathogenic features shown in neurodegenerative diseases.

Results and Discussion

Rational design consideration and characterization of chemical tools for regulating AD-related pathological factors

To develop small molecules able to interact with distinct and interrelated targets (i.e., metals, metal-free A β , metal-A β , ROS, free organic radicals) and modulate their reactivities (i.e., peptide aggregation, generation of toxic peptide conformations, oxidative stress), a library of small molecules was rationally designed based on the previously reported metal-A β -interacting framework (**L2-b**,^[7] Table 1). In our initial studies of **1–4** (Table 1), the electron-donating properties of the aniline (in **1**) and dimethylamine (in **3**) groups were suggested to be important in the formation of their radical forms required for activity toward their targets.^[5] In our complete chemical series, new compounds (**5–9**; Table 1) were included to contain electron-donating or electron-withdrawing groups to tune ionization potentials (IPs) of the basic framework affording distinct activities with targets: 1) a diethylamino (for **5**) or 4-morpholino (for **6**) group was installed in **5** and **6**, respectively, compared with the dimethylamino component of **8**, **9**, and **L2-b**; 2) compound **7**, composed of an electron-withdrawing nitro moiety, was constructed to decrease the compound's ability to oxidize similar to **2**,^[5] which contains a 3,5-dimethoxybenzene moiety and is relatively stable even in the presence of Cu^{II}. These compounds were relatively easily obtained and purified (see Supporting Information).

To confirm our rational design principle, computational calculations were first performed to predict the first and second electron ionization potentials (IP₁ and IP₂, respectively) of the two-electron oxidation of our compounds (**1–9**) as a method to compare their relative ability to undergo oxidation. As summarized in Table 1, the compounds (**5**, **6**, **8**, and **9**) designed to undergo oxidation have similar or lower computed IPs to the previously determined values for **1**,^[5] **3**,^[5] **4**,^[5] and **L2-b**^[8] suggesting that **1**, **3–6**, **8**, and **9** can produce radicals to be necessary for activity. Furthermore, as expected, the computational studies indicate that **7**, along with **2**, are more difficult to be oxidized than the other compounds (Table 1). To experimentally support these computational findings, the electrochemical behavior of **1–9** was probed by cyclic voltammetry in dimethyl sulfoxide (DMSO). All compounds with the exception of **1** and **7** showed single irreversible oxidation waves (Figure 1). Compound **1** exhibited two irreversible oxidation waves with peak anodic potentials of 0.262 and 0.521 V (at a scan rate of 250 mV s⁻¹), respectively (Figure 1 and Figure S1 in the Supporting Information). Due to the irreversible nature of the electrochemical waves in DMSO, $E_{1/2}$ values could not be obtained; however, the peak anodic potentials of compounds **1**, **3–6**, **8**, and **9** occurred at much lower potentials (i.e., 0.262, 0.284, 0.240, 0.228, 0.388, 0.286, and 0.238 V, respectively, at a scan rate of 250 mV s⁻¹) than that of **2** (i.e., 0.923 V at a scan rate of 250 mV s⁻¹) (Figure 1 and Table S1 in the Supporting Information). Compound **7** did not exhibit any oxidation waves over a potential window of -0.20 to 1.4 V. The compounds (i.e., **1**, **3–6**, **8**, and **9**) that are more easily oxidized have peak anodic po-

tentials compared to a water-soluble analogue of vitamin E, Trolox (~0.3 V),^[9a] as well as a structurally similar compound, *p*-phenylenediamine (~0.4 V).^[9b,c] Likewise, the compounds, i.e., **2** and **7**, that are more difficult to oxidize have higher peak anodic potentials more similar to acetaminophen (~0.6 V).^[9d] As a way to compare **1–9** to other compounds, we also employed the commonly used the Trolox Equivalence Antioxidant Capacity (TEAC) assay (see below), directly correlated to the activity of Trolox.^[5] Overall, our electrochemical studies are consistent with our calculation predictions that **2** and **7** are relatively more difficult to oxidize than **1**, **3–6**, **8**, and **9**; thus, they are less likely to generate the radical form required for reactivity with metal-free A β and metal-bound A β species.

In addition, because the oxidation of our compounds is associated with their binding to Cu^{II}, as indicated from our previous report,^[5] **8** and **9** were constructed to modulate metal binding affinities to allow for more control of their activity. The steric hindrance from the methyl group on the bridging carbon of **8** can cause the pyridyl nitrogen and the secondary amine to align to provide a metal binding site, affording enhanced metal binding. Compound **3** with a quinoline group can have a slightly lower metal binding affinity than the compounds containing a pyridine moiety, while **9** was designed with a methylimidazole moiety to have a stronger metal binding affinity, on the basis of their relative Lewis basicities as reflected in their p*K*_a values.^[10]

Furthermore, the ability for small molecules to passively diffuse across the blood–brain barrier (BBB) was also considered in our tool design. The BBB permeability of **1–9** was predicted by adhering to Lipinski's rules, along with calculated logBB values, as well as using the in vitro parallel artificial membrane permeability assay adapted for assessing BBB permeability (PAMPA-BBB). All values for **1–9** were then compared with that of **L2-b** (Table S2 in the Supporting Information).^[5,7b] The overall data indicate that our compounds can passively diffuse across the BBB, suggesting their potential application in the brain as chemical tools.

Modulation of metal-free A β and metal-A β aggregation

The ability of **1–9** to prevent A β aggregation (inhibition experiment; Figure 2 and Figure S2 in the Supporting Information) and disassemble preformed A β aggregates (disaggregation experiment; Figures S3 and S4 in the Supporting Information) in the absence and presence of metal ions [i.e., Cu^{II} and Zn^{II}] were evaluated at both short (4 h) and longer (24 h) incubation time points. Note that **1–4** were previously studied only after the 24 h incubation time^[5] and the new results of **1–4** at the 4 h incubation time interval were included in this present work for the purpose of a comprehensive comparison with those of the other compounds. Two isoforms of A β (A β ₄₀ and A β ₄₂) were used for our studies because their aggregation pathways have been suggested to occur through different mechanisms.^[11] Size distributions and morphologies of the resulting A β species were analyzed by gel electrophoresis followed by western blot analysis (gel/western blot) and transmission electron microscopy (TEM), respectively.

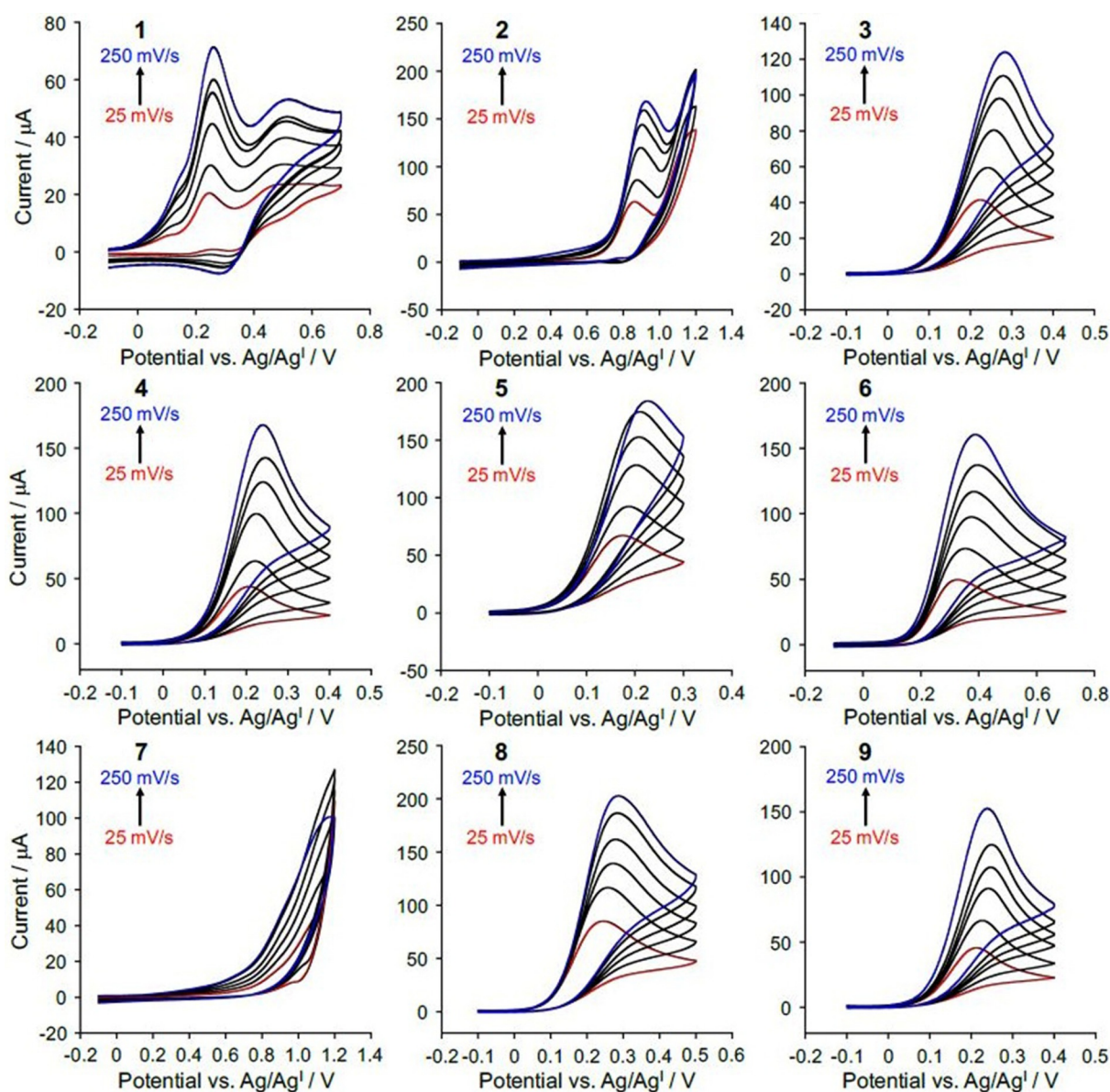


Figure 1. Electrochemical analysis of 1–9. Cyclic voltammograms of 1–9 (1 mM) were recorded in DMSO with 0.1 M $(\text{Bu}_4\text{N})(\text{ClO}_4)$ as a supporting electrolyte at scan rates of 25, 50, 100, 150, 200, and 250 mV s^{-1} at room temperature under $\text{N}_2(\text{g})$. The electrochemical parameters from the voltammograms are reported in Table S1.

Compound **4** was found to be the only molecule capable of interacting with both metal-free and metal-associated $\text{A}\beta$ with more noticeable changes effected at the shorter time point (4 h incubation) in metal-free $\text{A}\beta_{42}$ inhibition experiments and $\text{A}\beta_{40}$ disaggregation experiments (Figure 2; Figures S2–S4 in the Supporting Information). For **3**, **5**, and **9**, the aggregation of $\text{Cu}^{\text{II}}\text{-A}\beta$ and $\text{Zn}^{\text{II}}\text{-A}\beta$ was redirected selectively over metal-free $\text{A}\beta$ aggregation. Additionally, these compounds had a stronger effect at later time points with their activity toward $\text{Zn}^{\text{II}}\text{-A}\beta$ being negligible at the early incubation time point. This is similar to the previously reported activity of **L2-b**.^[7] Compounds **1**, **2**, and **6** could only modulate $\text{Cu}^{\text{II}}\text{-A}\beta$ aggregation to different extents. Compound **1** has a more noticeable effect on $\text{Cu}^{\text{II}}\text{-A}\beta$ aggregation at the longer time point (24 h incubation) while **6** influences $\text{Cu}^{\text{II}}\text{-A}\beta$ aggregation more noticea-

bly at 4 h in both inhibition and disaggregation experiments (Figure 2; Figures S2–S4 in the Supporting Information). Compound **8** is shown to have the unique activity of having a more prominent action at the earlier incubation time point toward $\text{Cu}^{\text{II}}\text{-A}\beta$ aggregation in the inhibition experiments but the opposite occurred in the disaggregation experiments where its ability to break up preformed $\text{Cu}^{\text{II}}\text{-A}\beta$ aggregates was more detectable after 24 h. In addition, **8** is indicated to have influence on preformed $\text{Zn}^{\text{II}}\text{-A}\beta$ aggregates upon 24 h incubation (Figure S4 in the Supporting Information). In both the inhibition and disaggregation experiments, **2** does not have a prominent effect on $\text{Cu}^{\text{II}}\text{-A}\beta$ aggregation with a stoichiometric ratio of Cu^{II} and $\text{A}\beta$; however, previous studies^[5] indicate that **2** could control $\text{Cu}^{\text{II}}\text{-A}\beta$ aggregation at higher Cu^{II} concentrations. Compound **7** also does not have significant effects on metal-

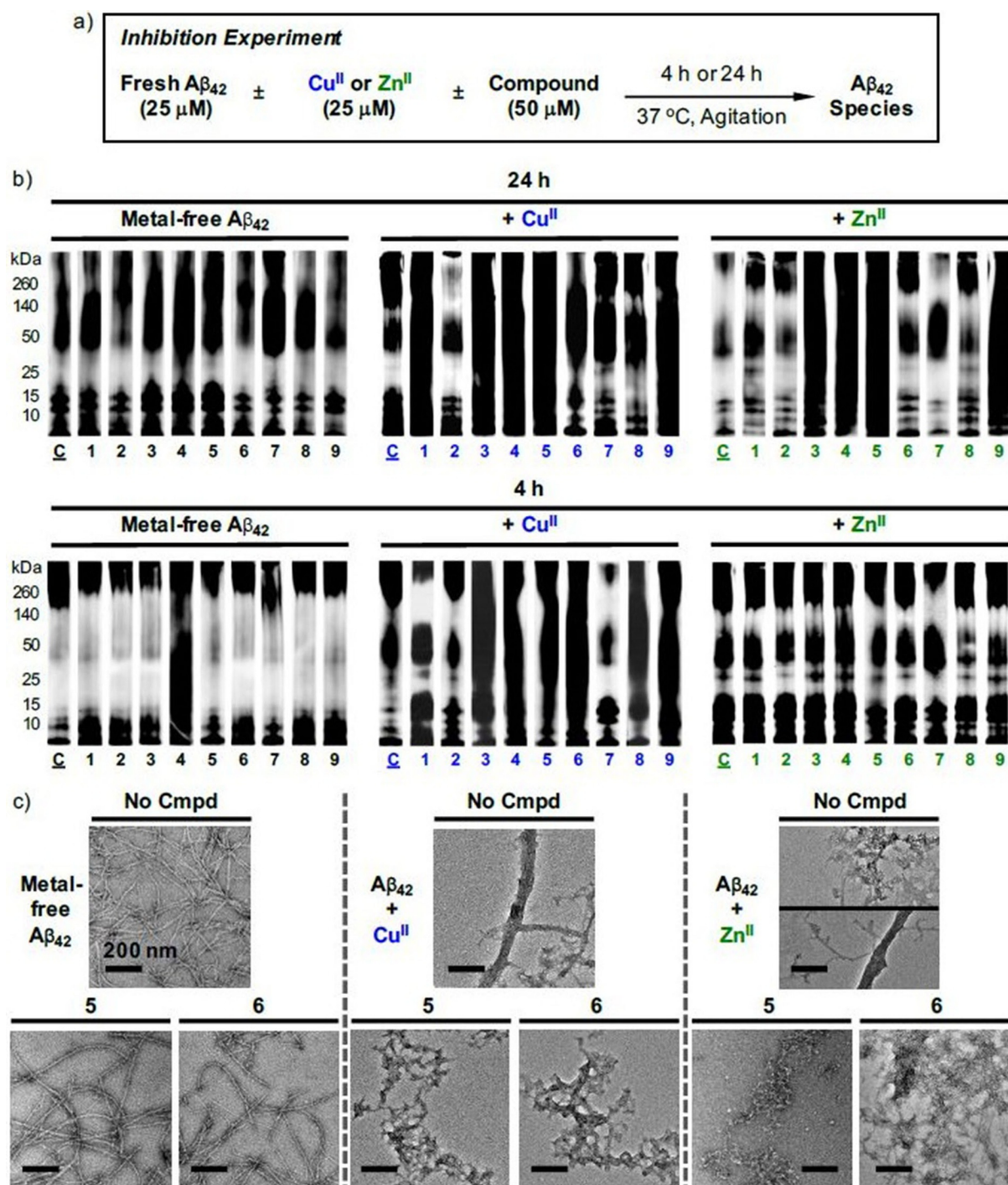


Figure 2. Modulation of $A\beta_{42}$ aggregation by 1–9. a) Scheme of inhibition experiments. Mixtures of freshly prepared $A\beta$ with or without Cu^{II} (blue) or Zn^{II} (green) were treated with 1–9 and incubated for 4 or 24 h before analysis. $A\beta$ samples excluding compounds (lane C) were also prepared as controls. Conditions: $[A\beta_{42}] = 25\ \mu\text{M}$; $[\text{Cu}^{\text{II}} \text{ or } \text{Zn}^{\text{II}}] = 25\ \mu\text{M}$; [compound] = 50 μM ; pH 6.6 (for Cu^{II} -containing samples) or pH 7.4 (for metal-free and Zn^{II} -containing samples); 37°C ; constant agitation. b) Analysis of the molecular weight of the resultant $A\beta$ species after 4 or 24 h incubation in the absence (left) or presence of Cu^{II} (middle) or Zn^{II} (right) by gel electrophoresis and subsequent western blotting (gel/western blot) with an anti- $A\beta$ antibody (6E10). c) TEM images of the $A\beta$ aggregates before (top) and after treatment with 5 and 6 (bottom) (scale bar = 200 nm).

free and metal- $A\beta$ aggregation (Figure 2; Figures S2–S4 in the Supporting Information). Unlike 2, however, even at higher Cu^{II} and Zn^{II} concentrations, 7 does not have an apparent influence on both metal-free and metal-induced $A\beta$ aggregation (Figure S5 in the Supporting Information).

TEM studies were carried out to visualize the morphology of the resulting $A\beta$ aggregates after 24 h incubation with 5, 6, and 8. These compounds were chosen for the further TEM analysis based on their differing activity toward metal-free and metal- $A\beta$ in the gel/western blot experiments. Compounds 5

and **8** are shown to react with metal-A β while **6** is specific for Cu^{II}-A β . In agreement with the gel/western blot experiments, **5** does not have an impact on the A β forms in the absence of metal ions. In the presence of Cu^{II} and Zn^{II}, however, **5** produces less structured, more amorphous A β aggregates (Figure 2; Figures S2–S4 in the Supporting Information). Similar results were obtained in the metal-free and Cu^{II} samples containing **6**; however, there was not a significant effect on the A β species present in the Zn^{II}-containing samples. In the case of **8**, TEM was only conducted on the **8**-treated Cu^{II}-A β samples to help understand the difference in the varied reactivity in both inhibition and disaggregation experiments (see above). Despite showing limited activity in the gel/western blot studies from the 24 h inhibition samples, long and thick fibrils, indicated in the control samples, are not present after treatment with **8** (Figure S2 in the Supporting Information). This suggests that **8** could redirect peptides into larger species that cannot penetrate into the gels. While in disaggregation samples, where gel/western blots showed activity, **8** could mainly produce shorter fibrils (Figure S4 in the Supporting Information). As a whole, our peptide aggregation experiments demonstrate that our small molecules have varying abilities to control metal-free and metal-induced A β aggregation to different extents.

Molecular-level interactions with multiple amyloidogenic targets

Metal-free and Cu^{II}-treated A β monomers

¹⁵N-Labeled A β_{40} monomer was titrated with **1–9** (0 to 10 equiv) and monitored by two dimensional (2D) ¹H-¹⁵N band-selective optimized flip-angle short-transient (SOFAST)-heteronuclear multiple quantum coherence (HMQC) nuclear magnetic resonance (NMR) spectroscopy to observe the amino acid residues of A β that are targeted by **1–9** (Figure 3 and Figure S6 in the Supporting Information). From our 2D SOFAST-HMQC NMR results, **1–9** are shown to trigger relatively low chemical shift perturbations (CSPs), similar to the previous studies with **L2-b** and **L2-NO**,^[12] suggesting weak, nonspecific interactions with A β . This is also indicated for **4**, which does show the reactivity toward metal-free A β , suggesting that its hydrolysis to produce **DMPD**^[6] is required before interaction and subsequent aggregation modulation.^[5]

To explore the interactions between A β_{40} and **5–9**, nano-electrospray ionization-mass spectrometry (nESI-MS) combined with ion mobility-mass spectrometry (IM-MS), optimized for the detection of non-covalent protein complexes, was used.^[13] Data obtained from the Cu^{II}-treated peptide samples incubated with **5–9** for 30 min (37 °C), presented in Figure 4, indicated that **5**, **6** and **9** exhibited a metal-dependent interaction with A β_{40} . All three of these compounds were capable of producing Cu-ligand-dependent signals corresponding to a mass 89 Da lighter than the apo A β_{40} , with clear differences in product abundance, and are absent under the ligand-free conditions. These data are consistent with some small molecules reported previously.^[5,7a] In the absence of Cu^{II}, no evidence of the compounds' interactions was observed, which is in agreement with

the findings obtained from our aggregation experiments (Figure S7 in the Supporting Information). As expected from our gel/western blot studies (Figure 2; Figures S2–S5 in the Supporting Information), **7** is indicated to have no interactions with both metal-free A β and metal-A β , which could be related to its absence of noticeable anti-amyloidogenic activity in vitro. Along with other data presented here, these observations support that **8** likely targets higher order, more transient oligomeric species that cannot be resolved by IM-MS. Consistent with these observations, whilst attempts to observe Cu^{II}-small molecule-bound A β_{40} dimers were carried out, the data proved to be inconclusive due to poor signal-to-noise levels associated with increased metal adduct formation within the A β aggregate states.

Monomeric Zn^{II}-A β

Because **1**^[5] (only for Cu^{II}-A β) and **L2-b**^[7] (for both Cu^{II}- and Zn^{II}-A β) are demonstrated to bind Zn^{II} but have differing activities toward modulation of Zn^{II}-A β aggregation, their binding affinities (K_d) were compared. UV/Vis variable-pH spectrophotometric titrations were carried out with a mixture of Zn^{II} and **1** (Figure S8 in the Supporting Information). This titration experiment indicates the presence of a 1:1 complex under the experimental conditions having a stability constant ($\log\beta$) of 5.5(3). Based on this value and the previously determined pK_a values of **1**, the pZn ($pZn = -\log[Zn_{\text{unchelated}}]$) was calculated to be 5.5, which is an approximate disassociation constant (K_d , $10^{-5.5} \text{ M} \approx [Zn_{\text{unchelated}}]$) (Figure S8 in the Supporting Information). Compared to **1**, **L2-b** is shown to have an apparent K_d of $10^{-6.1} \text{ M}$ for Zn^{II} indicating the generation of 1:1 and 1:2 Zn^{II}-to-ligand complexes.^[7b] The high micromolar binding affinity of **1** for Zn^{II} is not enough to control Zn^{II}-A β aggregation, since A β itself is indicated to have the micromolar to nanomolar K_d for Zn^{II}.^[1a-c] As previously reported, the minimum binding affinity of small molecules for Zn^{II} is in the micromolar or lower range in order to control Zn^{II}-A β aggregation.^[1a-c] This is further supported by our previous studies with **2** which also does not modulate Zn^{II}-A β aggregation where the K_d for Cu^{II} is reported to be micromolar.^[5] It is expected that **2** would have an even lower affinity for Zn^{II} due to the trends observed in the Irving–Williams series.^[14] Thus, **2**, along with **1**, has a binding affinity for Zn^{II} that is too low to interact with Zn^{II}-A β .

2D SOFAST-HMQC NMR studies were conducted to further understand the interaction of **1**, **4**, and **5** with Zn^{II}-¹⁵N-labeled A β_{40} monomer (Figure 5 and Figure S9 in the Supporting Information). These compounds were chosen due to their differing abilities to interact with Zn^{II}-A β . Compound **1** was indicated to have limited reactivity toward Zn^{II}-A β , while **4** and **5** were shown to be able to redirect the aggregation of A β in the presence of Zn^{II} (see below). As expected, **1** does not demonstrate an ability to interact with Zn^{II}-A β as evidenced by limited changes in intensity upon treatment with the compound (Figure 5 and Figure S9 in the Supporting Information). Compound **4** also does not cause significant changes in the spectra, which could be due to this molecule having only a limited initial interaction with Zn^{II}-A β or its degradation. Interestingly,

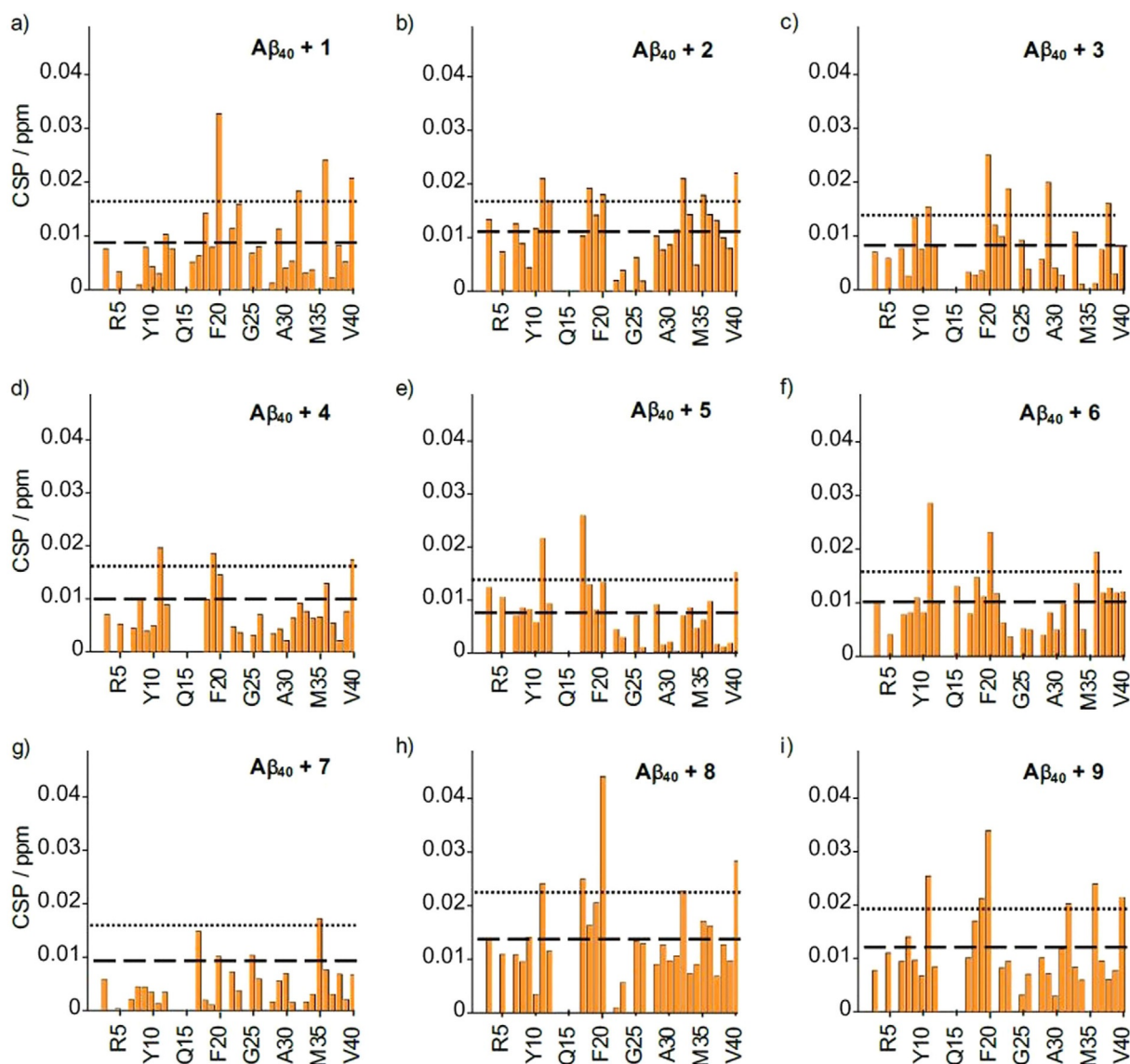


Figure 3. Interaction of 1–9 with monomeric $A\beta_{40}$, monitored by SOFAST-HMQC NMR. Normalized chemical shift perturbations (CSPs) of ^1H and ^{15}N amide atoms for $A\beta_{40}$ after addition of 10 equiv of compounds from the SOFAST-HMQC NMR (600 MHz) spectra (Figure S6). Two horizontal lines represent the average chemical shift (dashed line) plus one standard deviation (dotted line). Residues that show no CSP are the result of unresolved peaks in the spectra.

unlike the other compounds which are able to reverse the decrease in signal intensity caused by Zn^{II} -induced aggregation of $A\beta$, **5** had the opposite effect as addition to Zn^{II} - $A\beta$ further decreased the intensity of all residues. This could suggest that **5** may mediate the formation of NMR-invisible oligomers. This is in contrast to **L2-b** which demonstrates larger changes in the NMR spectra of Zn^{II} - $A\beta$ ^[7b,8] denoting that **L2-b** can directly interact with Zn^{II} - $A\beta$ possibly forming a ternary complex and subsequently control the Zn^{II} - $A\beta$ aggregation pathways.

Overall, the studies of our small molecules with Zn^{II} or Zn^{II} - $A\beta$ suggest that our compounds which do not modulate Zn^{II} - $A\beta$ aggregation (**1**, **2**, **6**, and **7**) do not have significant interactions with Zn^{II} - $A\beta$ most likely due to low binding affinities for Zn^{II} . In contrast, the compounds which have an effect on Zn^{II} - $A\beta$ aggregation (**3**, **5**, **8**, and **9**) could have the affinities for Zn^{II} , which directs the formation of ternary complexes with Zn^{II} - $A\beta$. In the case of **4**, this compound can undergo hydroly-

sis in the presence of Zn^{II} to produce **DMPD**,^[5,6] a known Zn^{II} - $A\beta$ -interacting compound.

Regulation of oxidative stress

The activity of **5**–**9** to mediate oxidative stress was investigated (Figure 6a,b). First, the ability to scavenge free organic radicals was examined using the TEAC assay^[5,7a,15] (Figure 6a). Compounds **5**, **6**, **8**, and **9** display a greater antioxidant capacity than Trolox [**5** and **9**, slightly higher (~1.5 and 1.7, respectively); **6** and **8**, much higher (~3.2 and 2.0, respectively)]. This is similar to the previously reported antioxidant capacities of **1**–**4**^[5] and **L2-b**.^[7a,12] Conversely, **7** is not found to have an effect toward free organic radicals (Figure 6a) which can be attributed to its absence of observable anodic waves over a large potential window and its high calculated IPs as shown in Figure 1 and Table 1, respectively.

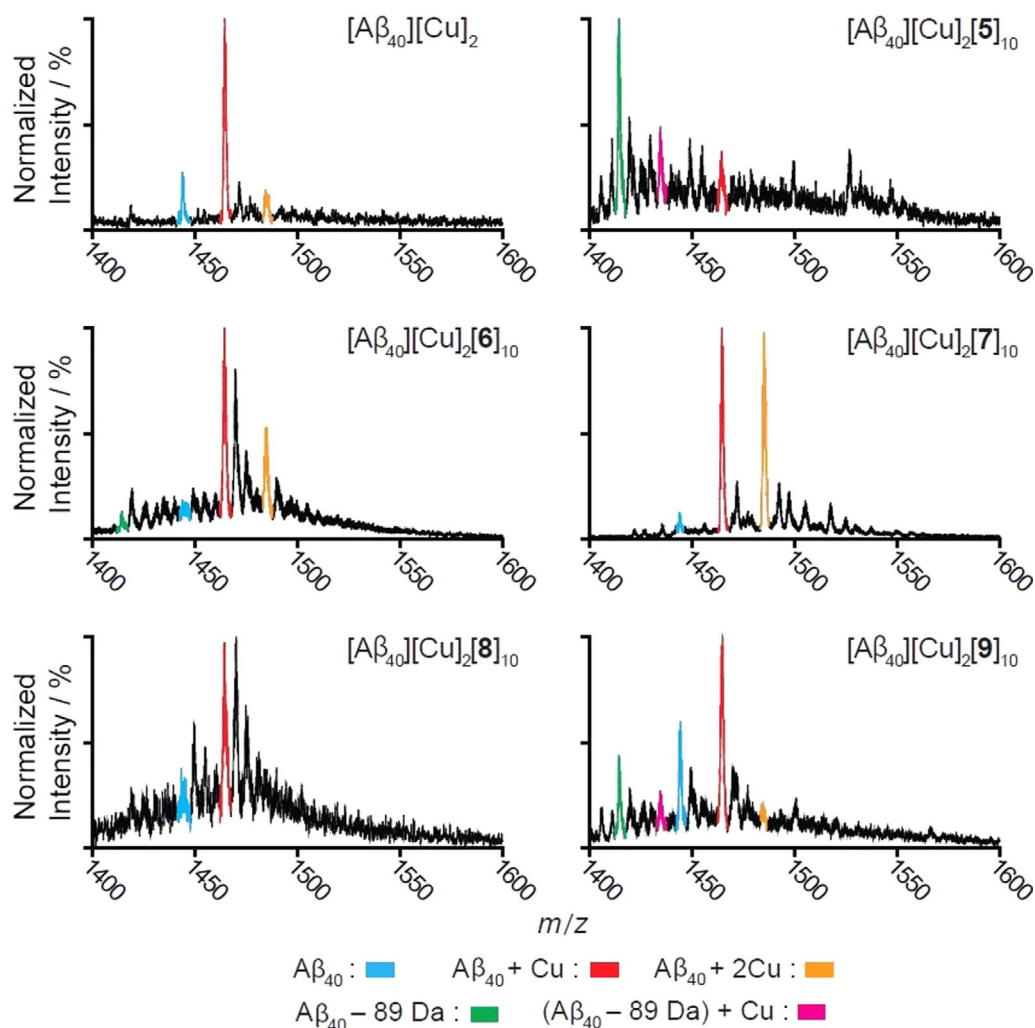


Figure 4. Mass spectrometric analysis of $A\beta_{40}$ incubated with 5–9 in the presence of Cu^{II} . The data show that relative to ligand-free conditions, 5, 6 and 9 are capable of covalently modifying $A\beta_{40}$ when incubated with Cu^{II} through their transient interactions with the N-terminus. No activity was observed in the absence of copper (Figure S7). Conditions: $[A\beta_{40}] = 20 \mu M$ (3+ charge state shown); $[compound] = 200 \mu M$; $[Cu^{II}] = 40 \mu M$.

The ability of 5–9 to decrease the production of ROS by Fenton-like reactions promoted by Cu^{II} was examined using the 2-deoxyribose assay (Figure 6b).^[16] Compounds 8 and 9 are found to better control the generation of hydroxyl radicals ($\cdot OH$) than the previously studied 1–3^[5] (~50% production inhibited) with 9 being the best compound studied (~75% production inhibited; Figure 6b). Compounds 5 and 7 have comparably lower abilities to prevent the formation of ROS being able to reduce the presence of $\cdot OH$ by only ~30 and 20%, respectively. Therefore, our small molecules are able to quench free organic radicals as well as control ROS generation.

Abatement of toxicity induced by metal-free and metal-treated $A\beta$

Based on the different activities toward redirection of metal-free $A\beta$ and metal- $A\beta$ aggregation and ability to mediate oxidative stress, 5–9 were chosen for further analysis of their toxicity in human neuroblastoma SK-N-BE(2)-M17 (M17) cells. Compounds 5 and 7 (20 μM) are found to decrease cell viability

by ~30% in the absence or presence of metal ions [Cu^{II} (20 μM) or Zn^{II} (20 μM)] (Figure 6c). Under the same conditions, 6, 8, and 9 are shown to be relatively nontoxic with 9 slightly decreasing cell viability to ~85% in the presence of Cu^{II} . Furthermore, 6, 8, and 9 are able to mitigate the toxicity of $A\beta_{40}$ (Figure 6d) and $A\beta_{42}$ (Figure 6e) in the absence (left) and presence of externally introduced Cu^{II} (middle) and Zn^{II} (right). Thus, 6, 8, and 9 are observed to reduce the cytotoxicity of metal- $A\beta$.

Conclusions

Inspired by initial studies regarding molecular modes of action of structurally similar compounds toward multiple factors (i.e., metals, metal-free $A\beta$, metal- $A\beta$, ROS, free organic radicals) involved in AD pathogenesis, a chemical library of small molecules was constructed to elucidate how structural variations could direct their regulatory activities for pathological targets. Our studies indicate the specificity for tempering the reactivity of Cu^{II} - $A\beta$ over Zn^{II} - $A\beta$ and metal-free $A\beta$ for 1, 2, and 6;

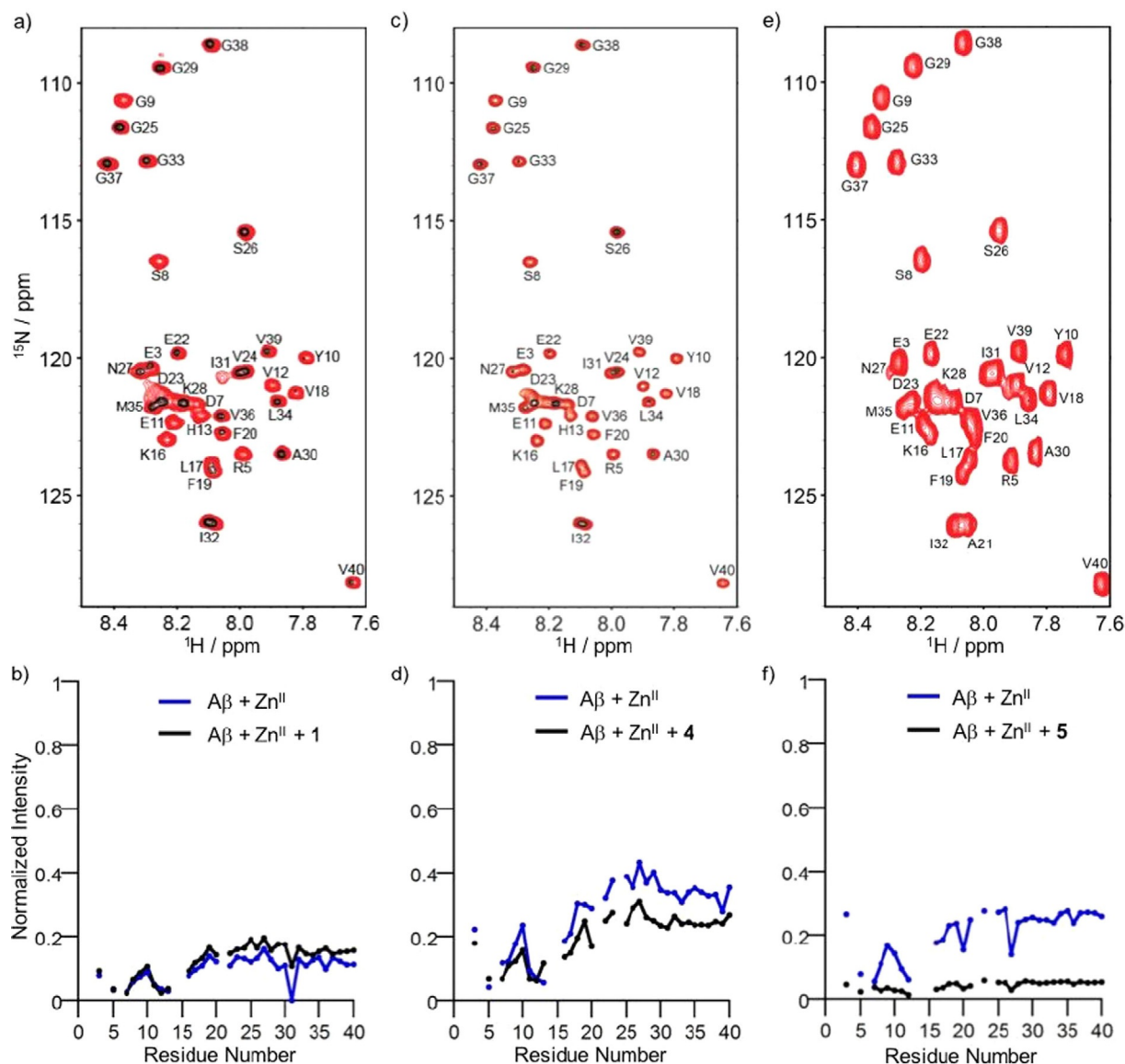


Figure 5. SOFAST-HMQC NMR (900 MHz) studies of compounds **1**, **4**, and **5** with ^{15}N -labeled $\text{A}\beta_{40}$ treated with Zn^{II} . a), c), e) Spectra of $\text{A}\beta_{40}$ (red) and after addition of Zn^{II} and compound (black). b), d), f) Intensities of $\text{A}\beta$ with Zn^{II} before (blue) and after addition of compound (black) normalized to the initial metal-free $\text{A}\beta_{40}$ signal. The spectra of ^{15}N -labeled $\text{A}\beta_{40}$ treated with Zn^{II} are presented in Figure S9.

metal- $\text{A}\beta$ versus metal-free $\text{A}\beta$ for **3**, **5**, **8**, **9**, and **L2-b**; no specificity for **4** (modulating with $\text{A}\beta$ regardless if metal ions are or are not present); having no detectable effects of **7** for both metal-free and metal-bound $\text{A}\beta$. We show that these reactivity behaviors can be imparted with consideration of the electrochemical characteristics and metal binding affinities of such small molecules. Furthermore, we present that these compounds have varying capabilities to diminish oxidative stress with **6** being the best antioxidant and **9** having the greatest control of ROS production from Fenton-like reactions, in contrast to **7** which has little antioxidant capacity and regulation of ROS formation. Additionally, the toxicity of metal-free $\text{A}\beta$ and metal- $\text{A}\beta$ was found to be diminished by **6**, **8**, and **9** in living cells.

Taken together, we demonstrate the feasibility of inventing chemical tools directed at investigating the involvement of

specific facets of AD through tuning their oxidation and metal binding properties. The knowledge gained from our complete studies using a series of small molecules (**1**–**9**) will aid in the development of novel chemical tools with optimal properties. These optimal characteristics, in addition to good pharmacological features, include metal binding affinities that are strong enough to interact with metal- $\text{A}\beta$ species but do not disrupt the activities of essential metalloproteins, the specificity for the particular metal ions of interest, as well as the ability to interact with metal-free and metal-bound $\text{A}\beta$ species. By developing methods to rationally generate chemical tools that have different capabilities and combinations of capabilities, a more complete chemical tool set can be developed for identifying the pathogenesis of neurodegenerative diseases at the molecular level.

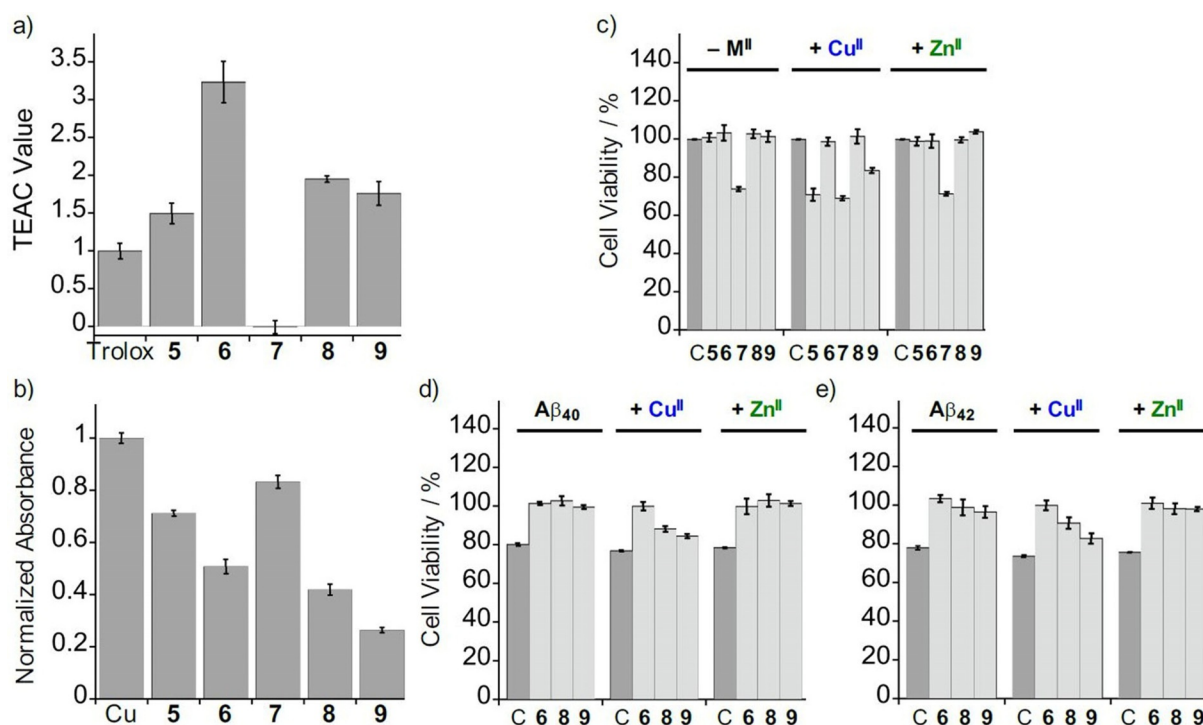


Figure 6. Abilities of compounds to mediate oxidative stress and regulate toxicity triggered by metal-free A β and metal-A β in living cells. a) Antioxidant activity of 5–9 in cell lysates, as evaluated by the TEAC assay. Values are relative to a vitamin E analogue, Trolox (6-hydroxy-2,5,7,8-tetramethylchroman-2-carboxylic acid). b) Capacity of 5–9 (125 μ M) toward control of Cu^{II}-triggered ROS production by Fenton-like reactions, as measured by the 2-deoxyribose assay ([Cu^{II}] = 10 μ M). c) Toxicity of 5–9 (20 μ M) and ability of 6, 8, and 9 to mediate the cytotoxicity of d) A β ₄₀ (20 μ M) and e) A β ₄₂ (20 μ M) in the absence (left) and presence of Cu^{II} (middle, 20 μ M) or Zn^{II} (right, 20 μ M) in M17 cells. C = Control samples without compound treatment. Percent cell viability was calculated relative to that of cells incubated only with DMSO (1% v/v). Error bars represent the standard error from three independent experiments ($p < 0.05$). Note that 5 and 7 were not studied with A β species due to relative toxicity with or without metal ions in the absence of A β .

Experimental Section

All reagents were purchased from commercial suppliers and used as received unless otherwise noted. A β ₄₀ and A β ₄₂ (the sequence of A β ₄₂: DAEFRHDSGYEVHHQKLVFFAEDVGSNKGAIIGLMVGGVVIA) were purchased from Anaspec Inc. (Fremont, CA, USA). Trace metals were removed from buffers and solutions used in A β experiments by treating with Chelex overnight (Sigma–Aldrich, St. Louis, MO, USA). Optical spectra were recorded on an Agilent 8453 UV-visible (UV/Vis) spectrophotometer. Absorbance values for biological assays, including cell viability and antioxidant assays, were measured on a Molecular Devices SpectraMax 190 microplate reader (Sunnyvale, CA, USA). ¹H and ¹³C 1D spectra were recorded using a 400 MHz Agilent NMR spectrometer. 2D NMR spectra were acquired on a Bruker Advance 600 MHz spectrometer equipped with a cryoprobe. More detailed experiments, including the preparation and characterization of the compounds, are described in the Supporting Information.

Acknowledgements

This work was supported by the Nine Bridges Program Research Fund and the Future-leading Specialized Research Fund (1.170051.01 and 1.170009.01) of UNIST (to M.H.L.); the National Research Foundation of Korea (NRF) grant funded by the Korean government [NRF-2016R1A5A1009405 and NRF-2017R1A2B3002585 (to M.H.L.); NRF-2014S1A2A2028270 (to

M.H.L. and A.R.)]; NIH (AG048934 to A.R.); and the University of Michigan Protein Folding Disease Initiative (to A.R., B.T.R., and M.H.L.). We thank Professor Kwang S. Kim for supporting the IP calculations. We also acknowledge Younwoo Nam, Milim Jang, and Jiyeon Han for initial analyses of TEM, biological activities, and electrochemistry, respectively.

Conflict of interest

The authors declare no conflict of interest.

Keywords: amyloid- β • free radicals • metal ions • small molecules • structure–activity relationships

- [1] a) K. P. Kepp, *Chem. Rev.* **2012**, *112*, 5193–5239; b) M. W. Beck, A. S. Pithadia, A. S. DeToma, K. J. Korshavn, M. H. Lim in *Ligand Design in Medicinal Inorganic Chemistry* (Ed.: T. Storr), Wiley, Chichester, **2014**, Chap. 10, pp. 256–286; c) M. G. Savelieff, A. S. DeToma, J. S. Derrick, M. H. Lim, *Acc. Chem. Res.* **2014**, *47*, 2475–2482; d) R. Jakob-Roetne, H. Jacobsen, *Angew. Chem. Int. Ed.* **2009**, *48*, 3030–3059; *Angew. Chem.* **2009**, *121*, 3074–3105; e) M. G. Savelieff, S. Lee, Y. Liu, M. H. Lim, *ACS Chem. Biol.* **2013**, *8*, 856–865; f) A. Corbett, J. Pickett, A. Burns, J. Corcoran, S. B. Dunnett, P. Edison, J. J. Hagan, C. Holmes, E. Jones, C. Katona, I. Kearns, P. Kehoe, A. Mudher, A. Passmore, N. Shepherd, F. Walsh, C. Ballard, *Nat. Rev. Drug Discovery* **2012**, *11*, 833–846; g) J. S. Derrick, M. H. Lim, *Chem-BioChem* **2015**, *16*, 887–898; h) M. Rowińska-Żyrek, M. Salerno, H. Kozłowski, *Coord. Chem. Rev.* **2015**, *284*, 298–312; i) A. D. Watt, V. L. Villeneuve, K. J. Barnham, *J. Alzheimer's Dis.* **2013**, *33*, S283–S293.

- [2] a) A. S. Pithadia, M. H. Lim, *Curr. Opin. Chem. Biol.* **2012**, *16*, 67–73; b) A. S. DeToma, S. Salamekh, A. Ramamoorthy, M. H. Lim, *Chem. Soc. Rev.* **2012**, *41*, 608–621; c) H. J. Lee, K. J. Korshavn, A. Kochi, J. S. Derrick, M. H. Lim, *Chem. Soc. Rev.* **2014**, *43*, 6672–6682; d) P. Faller, C. Hureau, *Chem. Eur. J.* **2012**, *18*, 15910–15920; e) P. Faller, C. Hureau, *Dalton Trans.* **2009**, 1080–1094; f) G. J. Siegel, N. Chauhan, A. G. Karczmar in *Exploring the Vertebrate Central Cholinergic Nervous System* (Ed.: A. G. Karczmar), Springer, Boston, **2007**, Chap. 10, pp. 597–656.
- [3] a) K. J. Barnham, C. L. Masters, A. I. Bush, *Nat. Rev. Drug Discovery* **2004**, *3*, 205–214; b) S. Ayton, P. Lei, A. I. Bush, *Free Radical Biol. Med.* **2013**, *62*, 76–89; c) P. Faller, C. Hureau, G. L. Penna, *Acc. Chem. Res.* **2014**, *47*, 2252–2259; d) M. A. Greenough, J. Camakaris, A. I. Bush, *Neurochem. Int.* **2013**, *62*, 540–555.
- [4] a) C. Rodríguez-Rodríguez, M. Telpoukhovskaia, C. Orvig, *Coord. Chem. Rev.* **2012**, *256*, 2308–2332; b) C.-Y. Wong, L.-H. Chung, L. Lu, M. Wang, B. He, L.-J. Liu, C.-H. Leung, D.-L. Ma, *Curr. Alzheimer Res.* **2015**, *5*, 439–444; c) S. L.-F. Chan, L. Lu, T. L. Lam, S.-C. Yan, C.-H. Leung, D.-L. Ma, *Curr. Alzheimer Res.* **2015**, *12*, 434–438; d) S. A. Funke, D. Willbold, *Curr. Pharm. Des.* **2012**, *18*, 755–767; e) Q. Nie, X.-G. Du, M.-Y. Geng, *Acta Pharmacol. Sin.* **2011**, *32*, 545–551; f) N. D. Prins, P. Scheltens, *Alzheimer's Res. Ther.* **2013**, *5*, 56; g) W. V. Graham, A. Bonito-Oliva, T. P. Sakmar, *Annu. Rev. Med.* **2017**, *68*, 413–430.
- [5] M. W. Beck, J. S. Derrick, R. A. Kerr, S. B. Oh, W. J. Cho, S. J. C. Lee, Y. Ji, J. Han, Z. A. Tehrani, N. Suh, S. Kim, S. D. Larsen, K. S. Kim, J.-Y. Lee, B. T. Ruotolo, M. H. Lim, *Nat. Commun.* **2016**, *7*, 13115.
- [6] J. S. Derrick, R. A. Kerr, Y. Nam, S. B. Oh, H. J. Lee, K. G. Earnest, N. Suh, K. L. Peck, M. Ozbil, K. J. Korshavn, A. Ramamoorthy, R. Prabhakar, E. J. Merino, J. Shearer, J.-Y. Lee, B. T. Ruotolo, M. H. Lim, *J. Am. Chem. Soc.* **2015**, *137*, 14785–14797.
- [7] a) M. W. Beck, S. B. Oh, R. A. Kerr, H. J. Lee, S. H. Kim, S. Kim, M. Jang, B. T. Ruotolo, J.-Y. Lee, M. H. Lim, *Chem. Sci.* **2015**, *6*, 1879–1886; b) J.-S. Choi, J. J. Braymer, R. P. R. Nanga, A. Ramamoorthy, M. H. Lim, *Proc. Natl. Acad. Sci. USA* **2010**, *107*, 21990–21995.
- [8] H. J. Lee, K. J. Korshavn, Y. Nam, J. Kang, T. J. Paul, R. A. Kerr, I. S. Youn, M. Ozbil, K. S. Kim, B. T. Ruotolo, R. Prabhakar, A. Ramamoorthy, M. H. Lim, *Chem. Eur. J.* **2017**, *23*, 2706–2715.
- [9] a) P. Jakubec, M. Bancirova, V. Halouzka, A. Lojek, M. Ciz, P. Denev, N. Cibicek, J. Vacek, J. Vostalova, J. Ulrichova, J. Hrbac, *J. Agric. Food Chem.* **2012**, *60*, 7836–7843; b) R. Male, R. D. Allendoerfer, *J. Phys. Chem.* **1988**, *92*, 6237–6240; c) A. S. Pavitt, E. J. Bylaska, P. G. Tratnyek, *Environ. Sci.: Processes Impacts* **2017**, *19*, 339–349; d) D. J. Miner, J. R. Rice, R. M. Riggan, P. T. Kissinger, *Anal. Chem.* **1981**, *53*, 2258–2263.
- [10] a) R. S. Hosmane, J. F. Liebman, *Struct. Chem.* **2009**, *20*, 693–697; b) B. Lenarcik, P. Ojczenasz, *J. Heterocycl. Chem.* **2002**, *39*, 287–290; c) K. L. Haas, K. J. Franz, *Chem. Rev.* **2009**, *109*, 4921–4960.
- [11] S. L. Bernstein, N. F. Dupuis, N. D. Lazo, T. Wyttenbach, M. M. Condron, G. Bitan, D. B. Teplow, J.-E. Shea, B. T. Ruotolo, C. V. Robinson, M. T. Bowers, *Nat. Chem.* **2009**, *1*, 326–331.
- [12] M. G. Savelieff, Y. Liu, R. R. P. Senthamarai, K. J. Korshavn, H. J. Lee, A. Ramamoorthy, M. H. Lim, *Chem. Commun.* **2014**, *50*, 5301–5303.
- [13] a) H. Hernández, C. V. Robinson, *Nat. Protoc.* **2007**, *2*, 715–726; b) G. R. Hilton, J. L. P. Benesch, *J. R. Soc. Interface* **2012**, *9*, 801–816; c) F. Lanucara, S. W. Holman, C. J. Gray, C. E. Eyers, *Nat. Chem.* **2014**, *6*, 281–294.
- [14] H. Irving, R. J. P. Williams, *J. Chem. Soc.* **1953**, 3192–3210.
- [15] S. Lee, X. Zheng, J. Krishnamoorthy, M. G. Savelieff, H. M. Park, J. R. Brender, J. H. Kim, J. S. Derrick, A. Kochi, H. J. Lee, C. Kim, A. Ramamoorthy, M. T. Bowers, M. H. Lim, *J. Am. Chem. Soc.* **2014**, *136*, 299–310.
- [16] L. K. Charkoudian, D. M. Pham, K. J. Franz, *J. Am. Chem. Soc.* **2006**, *128*, 12424–12425.

 Manuscript received: August 3, 2017

Revised manuscript received: September 4, 2017

Version of record online: October 9, 2017